A Density Functional Study of Nickel(II) Diimide Catalyzed Polymerization of Ethylene

Liqun Deng, Peter Margl, and Tom Ziegler*

Contribution from the Department of Chemistry, University of Calgary, 2500 University Drive, N.W., T2N 1N4 Calgary, Alberta, Canada

Received August 14, 1996. Revised Manuscript Received November 18, 1996[⊗]

Abstract: We have applied a nonlocal density functional method to the study of ethylene polymerization with a Ni(II) catalytic center coordinated to diimine (HN=CH−CH=NH). We have investigated chain initialization, chain propagation, as well as chain isomerization and chain termination. Chain initialization proceeds in a stepwise fashion, with an overall activation barrier of 11.1 kcal/mol. Chain propagation can proceed via two different pathways, which have similar activation energies (16.8 and 17.5 kcal/mol, respectively). In contrast to behavior observed for metallocene catalysts, none of the insertion transition states show agostic stabilization. The activation energy for chain isomerization is 12.8 kcal/mol, which proceeds via a concerted mechanism, rotating the chain and simultaneously abstracting the β-agostic hydrogen. Chain termination occurs via a stable hydride intermediate, which is formed with a barrier of 9.7 kcal/mol and decays into the termination product with a small activation energy of 1.7 kcal/mol. Production of experimentally observed high molecular weight polymers can only be explained by suppression of the chain termination transition state due to sterically demanding substituents on the diimine ligand.

1. Introduction

Recently, nitrogen-ligated Ni(II)- and Pd(II)-based catalysts have emerged as promising alternatives to traditional Ziegler−Natta systems as well as to the newly developed metallocene catalysts for ethylene and α-olefin polymerization.[1,2] Brookhart's group has shown that these catalysts are able to convert ethylene and α-olefins into high molar mass polymers with microstructures which are directly related to the steric bulk of the ancillary ligand.[1] This development is of twofold importance: firstly, late transition metal catalysts have hitherto only been able to oligomerize olefins[3−7] due to competing chain termination (i.e. β-hydride elimination), whereas the new catalysts are highly active and produce high molecular weight polymers,[1] comparable to those of metallocene catalysts used in some commercial polyolefin processes. Secondly, polymer branching can be controlled by varying temperature, ethylene pressure, and steric bulkiness of the auxiliary ligand, which opens up numerous possibilities of tailored polymers.[1]

The mechanistic details of nickel(II) and palladium(II) diimine catalyzed ethylene polymerization have recently been studied by Brookhart's group.[1] The reaction mechanism determined by Johnson et al.[1] calls for a precatalyst (e.g. the diimide dimethyl complex) to be activated by a co-catalyst, resulting in formation of a diimide methyl complex (Figure 1). Once activation has occurred, (i) chain initialization proceeds via uptake of an olefin into the free site of the square-planar metal center and insertion of the coordinated olefin into the M−CH₃ (M = Ni, Pd) bond (Figure 1; S1). (ii) Chain propagation
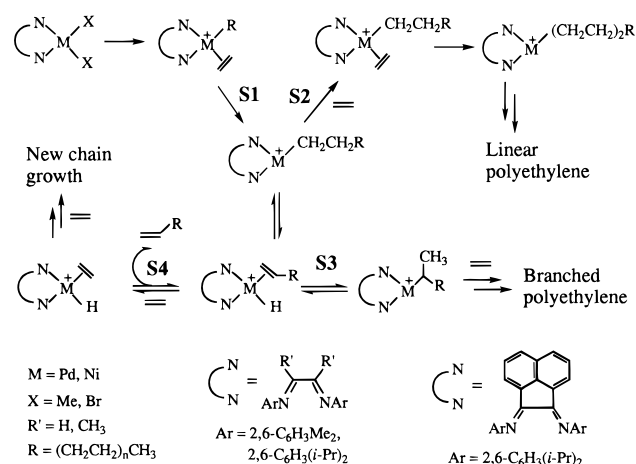
Figure 1. Flow chart of the chain initialization (S1), chain propagation (S2), chain isomerization (S3), and chain termination (S4) processes. Olefin hydrido species are shown for the sake of clarity, although they do not represent stable minima on the potential surface.

proceeds by coordination of free olefin and insertion into the M−R bond (R = growing chain) (Figure 1; S2). (iii) Chain isomerization happens by β-elimination of hydrogen from the growing chain and rotation of the chain by 180° around the M−olefin bond, followed by reattachment of the hydrogen to the terminal carbon atom (Figure 1; S3). (iv) Chain termination occurs by ethylene-assisted β-hydrogen elimination from the growing chain and transfer of the eliminated hydrogen to a coordinating olefin (Figure 1; S4).

Although many mechanistic details of the process are fairly well established,[1] to our knowledge no theoretical investigation has been performed yet to elucidate its energetics and kinetics. It is our goal here to apply density functional theory to shed light on the mechanistic details of the Ni(II)-catalyzed polymerization of ethylene. We model the catalytic center by Ni(II) coordinated to diimine (HN=CH−CH=NH), which is used to mimic the more sterically hindered substituted diimine ligands (Figure 1) of the original study by Johnson et al.[1]

In the present study, we focus exclusively on the generic

⊗ Abstract published in *Advance ACS Abstracts,* January 1, 1997.
(1) Johnson, L. K.; Mecking, S.; Brookhart, M. *J. Am. Chem. Soc.* **1996**, *118*, 267.
(2) Johnson, L. K.; Killian, C. M.; Brookhart, M. *J. Am. Chem. Soc.* **1995**, *117*, 6414.
(3) Keim, W. *Angew. Chem., Int. Ed. Engl.* **1990**, *29*, 235.
(4) Brown, S. J.; Masters, A. F. *J. Organomet. Chem.* **1989**, *367*, 371.
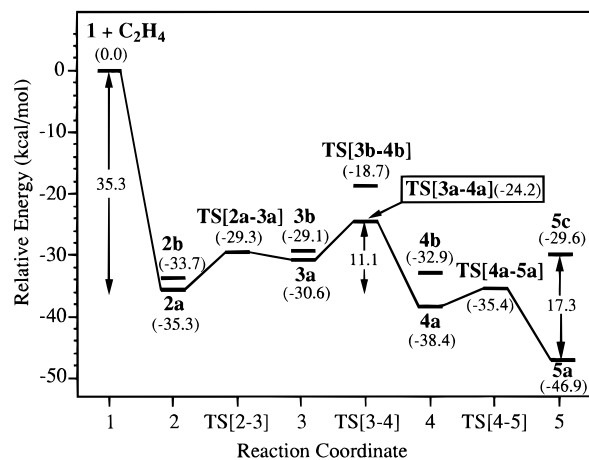(5) Keim, W.; Schulz, R. P. *J. Mol. Catal.* **1994**, *92*, 21.
(6) Abeywickrema, R.; Bennett, M. A.; Cavell, K. J.; Kony, M.; Masters, A. F.; Webb, A. G. *J. Chem. Soc., Dalton Trans.* **1993**, 59.
(7) Foulds, G. A.; Bennett, A. M. A.; Thornton, D. A.; Brown, S. J.; Clutterbuck, L. M.; Hinton, C.; Humphrey, G. B.; Masters, A. F. *Polyhedron* **1992**, *11*, 1285.

aspects of the polymerization process, neglecting the influence of the bulky ligands. Once the shape of the generic energy surface is known, the perturbation caused by the bulky ligands can readily be incorporated using combined quantum mechanical/molecular mechanical (QM-MM) techniques which are able to treat steric bulk more efficiently than pure QM methods. QM-MM calculations to that effect are in progress at our laboratory.

2. Computational Details

Stationary points on the potential energy surface were calculated with the program ADF, developed by Baerends[8,9] *et al.*, and vectorized by Ravenek.[10] The numerical integration scheme applied for the calculations was developed by te Velde[11,12] *et al.* The geometry optimization procedure was based on the method due to Versluis[13] and Ziegler. The electronic configurations of the molecular systems were described by a triple-ζ basis set on nickel[14,15] for 3s, 3p, 3d, 4s, and 4p. Double-ζ STO basis sets were used for carbon (2s, 2p), hydrogen (1s), and nitrogen (2s, 2p), augmented with a single 3d polarization function except for hydrogen where a 2p function was used. The $1s^2 2s^2 2p^6$ configuration on nickel and the $1s^2$ shell on carbon and nitrogen were assigned to the core and treated within the frozen core approximation. A set of auxiliary[16] s, p, d, f, and g STO functions, centered on all nuclei, was used in order to fit the molecular density and present Coulomb and exchange potentials accurately in each SCF cycle. Energy differences were calculated by augmenting the local exchange-correlation potential by Vosko[17] *et al.* with Becke's[18] nonlocal exchange corrections and Perdew's[19,20] nonlocal correlation correction. Geometries were optimized including nonlocal corrections. First-order scalar relativistic corrections[21-23] were added to the total energy, since a perturbative relativistic approach is sufficient for 3d metals. In view of the fact that all systems investigated in this work show a large HOMO-LUMO gap, a spin-restricted formalism was used for all calculations. All structures shown correspond to minimum points on the potential surface, except those prefixed by **TS**, which represent transition states. Transition states were obtained by full transition state optimization of structures obtained from linear transit calculations, until the Hessian had only one imaginary eigenvalue. No symmetry constraints were used, except where explicitly indicated. Saddle point determinations were initialized by a linear transit search from reactant to product along an assumed reaction coordinate. In each step along the reaction coordinate all other degrees of freedom were optimized. Full transition state optimizations were carried out on the geometries obtained by linear transit, except on transition state **TS[7a-12]**, whose potential surface proved to be too flat to be tractable by a transition state search based on the Hessian. This transition state will be discussed separately. We have recently verified the accuracy of our nonlocal DFT approach for barrier heights in a very similar Pd(II) system, where

(8) Baerends, E. J. Ph.D. Thesis, Free University, Amsterdam, The Netherlands, 1973.

(9) Baerends, E. J.; Ellis, D. E.; Ros, P. *Chem. Phys.* **1973**, *2*, 41.

(10) Ravenek, W. In *Algorithms and Applications on Vector and Parallel Computers*; te Riele, H. J. J., Dekker, T. J., van de Horst, H. A., Eds.; Elsevier: Amsterdam, The Netherlands, 1987.

(11) te Velde, G.; Baerends, E. J. *J. Comput. Chem.* **1992**, *99*, 84.

(12) Boerrigter, P. M.; te Velde, G.; Baerends, E. J. *Int. J. Quantum Chem.* **1988**, *33*, 87.

(13) Versluis, L.; Ziegler, T. *J. Chem. Phys.* **1988**, *88*, 322.

(14) Snijders, J. G.; Baerends, E. J.; Vernooijs, P. *At. Nucl. Data Tables* **1982**, *26*, 483.

(15) Vernooijs, P.; Snijders, J. G.; Baerends, E. J. *Slater Type Basis Functions for the Whole Periodic System*; Internal report (in Dutch); Department of Theoretical Chemistry, Free University: Amsterdam, The Netherlands, 1981.

(16) Krijn, J.; Baerends, E. J. *Fit Functions in the HFS Method*; Internal Report (in Dutch); Department of Theoretical Chemistry, Free University: Amsterdam, The Netherlands, 1984.

(17) Vosko, S. H.; Wilk, L.; Nusair, M. *Can. J. Phys.* **1980**, *58*, 1200.

(18) Becke, A. *Phys. Rev. A* **1988**, *38*, 3098.

(19) Perdew, J. P. *Phys. Rev. B* **1986**, *34*, 7406.

(20) Perdew, J. P. *Phys. Rev. B* **1986**, *33*, 8822.

(21) Ziegler, T.; Tschinke, V.; Baerends, E. J.; Snijders, J. G.; Ravenek, W. *J. Phys. Chem.* **1989**, *93*, 3050.

(22) Snijders, J. G.; Baerends, E. J. *Mol. Phys.* **1978**, *36*, 1789.

(23) Snijders, J. G.; Baerends, E. J.; Ros, P. *Mol. Phys.* **1979**, *38*, 1909.

Figure 2. Energy profile for the chain-initialization process. Different isomers of the same species are indicated by alphanumerics. All energies are in kcal/mol.

we concluded that barrier heights are systematically underestimated by only 3–5 kcal/mol.[24,25] Stanton and Merz have undertaken a systematic study of the reliability of DFT calculations for barrier heights and have concluded that nonlocal DFT yields results of the same quality as post-HF calculations.[26] In a number of previous papers, transition metal−ligand dissociation energetics have been proven to be correct within 5 kcal/mol of the experimental result.[27-31]

3. Results and Discussion

a. Chain Initialization. Chain initialization proceeds in a barrierless fashion by coordination of ethylene into the vacant square-planar site of the methyl precursor **1**, forming the ethylene π-complex **2a** in a reaction which is exothermic by 35.3 kcal/mol (Figure 2). A square-planar configuration is expected for a 4-coordinated d^8-system such as Ni(II) from simple orbital interaction considerations.[32] The ethylene in **2a** is rotated out of the molecular plane to reduce steric repulsion. Starting from **2a**, insertion of the ethylene into the Ni−methyl bond procceeds via rotation of the ethylene moiety into the molecular plane. The transition state **TS[2a−3a]** associated with the rotation of the olefin lies 6 kcal/mol above **2a**. The product of this rotation is the stable in-plane π-complex **3a**, which lies 4.7 kcal/mol above **2a**. However, due to the small barrier for the reverse reaction **3a** $\rightarrow$ **2a** (1.3 kcal/mol), one can expect **3a** to be negligibly populated. Decrease of the methyl−ethylene distance brings about the transition state for insertion **TS[3a−4a]** (11.1 kcal/mol above **2a**). Relaxation of **TS[3a−4a]** to the product side yields the kinetic insertion product **4a**, which exhibits strong η^2-γ-agostic bonding via the terminal methyl hydrogens. Conversion of **4a** into the final β-agostic thermodynamic product **5a** proceeds by twisting the C_α−C_β bond. The reorganization transition state **TS[4a−5a]** (3 kcal/mol above **4a**) breaks C_s symmetry and has only one γ-agostic interaction. We can give a lower limit of 17.3 kcal/mol for the β-agostic bond strength in **5a** by comparing its energy to **5c**, where the β-agostic bond is replaced by two much weaker (agostic distance 2.207 Å) α-agostic ones. The ther-

(24) Margl, P. M.; Ziegler, T. *J. Am. Chem. Soc.* **1996**, *118*, 7337.

(25) Margl, P.; Ziegler, T. *Organometallics* In press.

(26) Stanton, R. V.; Merz, K. M. J. *J. Chem. Phys.* **1993**, *100*, 434.

(27) Folga, E.; Ziegler, T. *J. Am. Chem. Soc.* **1993**, *115*, 5169.

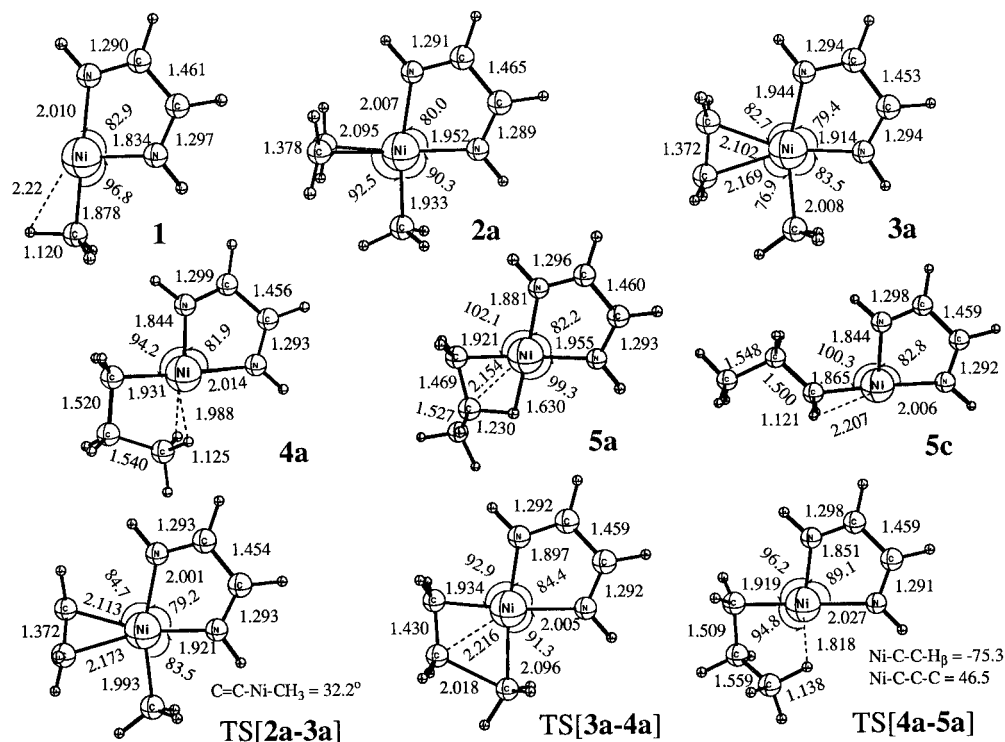(28) Li, J.; Schreckenbach, G.; Ziegler, T. *J. Phys. Chem.* **1994**, *98*, 4838.

(29) Li, J.; Schreckenbach, G.; Ziegler, T. *J. Am. Chem. Soc.* **1995**, *117*, 486.

(30) Ziegler, T.; Li, J.; Schreckenbach, G. *Inorg. Chem.* **1995**, *34*, 3245.

(31) Ziegler, T.; Li, J. *Can. J. Chem.* **1994**, *72*, 783.

(32) Albright, T. A.; Burdett, J. K.; Whanbgo, M.-H. *Orbital Interactions in Chemistry*; John Wiley & Sons: New York, 1985.
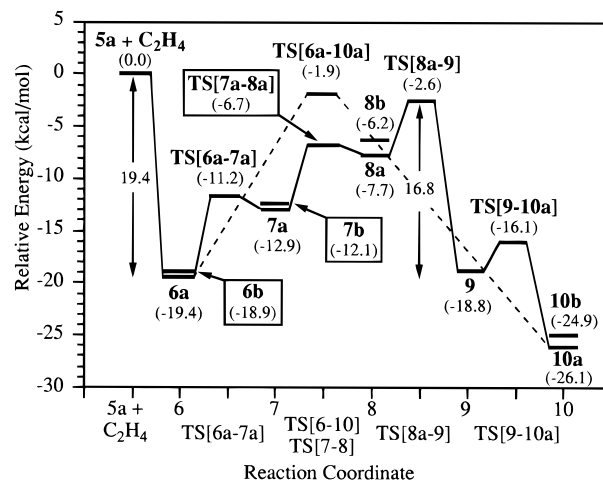
Chart 1

modynamic driving force of ethylene insertion relative to the π-complex **2a** is 11.6 kcal/mol, the barrier associated with insertion is 11.1 kcal/mol.

In order to complete the picture of the potential surface for chain initialization, we located the stationary points **2b**, **3b**, **TS-[3b−4b]**, and **4b**, which are analogous to **2a**, **3a**, **TS[3a−4a]**, and **4a** except that the methyl group is rotated into an eclipsed conformation relative to the ethylene moiety. As expected, the energy of the "**b**" conformers is generally higher than of their "**a**" counterparts due to increased steric repulsion (Figure 2). The larger energy gaps between **TS[3a−4a]/TS[3b−4b]** (5.5 kcal/mol) and **4a/4b** (5.5 kcal/mol) as compared to **2a/2b** (1.6 kcal/mol) and **3a/3b** (1.5 kcal/mol) indicate that the steric repulsion between ethylene and CH$_3$ hydrogens becomes more crucial as the C$_2$H$_4$−CH$_3$ distance shrinks. Since the "**b**" isomers are obviously not part of the minimum energy reaction path, we did *not* verify their true character as either minima or transition states in terms of the number of imaginary eigenvalues of the hessian.

b. Chain Propagation. Propagation of the chain commences with uptake of an ethylene unit by **5a** (Figure 3). Linear transit calculations show that attack from the top as well as laterally (from the direction of the β-agostic bond) proceeds without barrier to the trigonal bipyramidal ethylene π-complex **6a**, which lies 19.4 kcal/mol below **5a** + C$_2$H$_4$. This is in agreement with previous calculations on a similar Pd(II) system (H$_2$PCHCHPH$_2$Pd^{II}C$_2$H$_5$$^+$) which have also shown no barrier for ethylene uptake.[24] In **6a**, the β-agostic interaction is not broken; however, it is weakened by competing for electron density with the ethylene moiety. In H$_2$PCHCHPH$_2$Pd^{II}C$_2$H$_5$$^+$, where β-agostic bonding is weaker and the metal−ethylene bond stronger, the β-agostic bond of the ethyl group was destroyed by ethylene uptake.[24] The subsequent insertion process can proceed in two different fashions, depending on the orientation of the propyl chain: In the first instance, insertion proceeds directly by shrinking the distance between ethylene and the C$_\alpha$ atom of the propyl chain. This leads without further stable intermediates to a transition state **TS[6−10a]**, which occurs

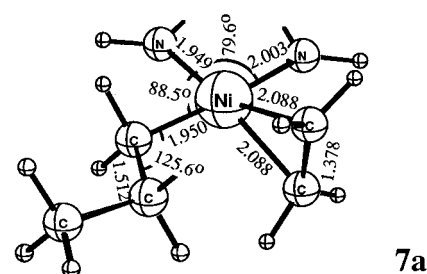**Figure 3.** Energy profile for the chain-propagation process. Conventions as in Figure 2.
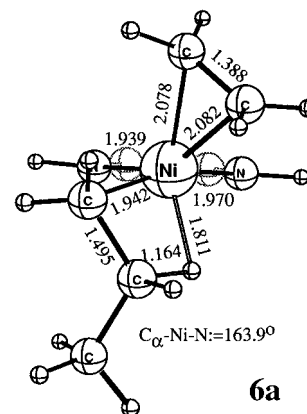
at a C(propyl)$_\alpha$−C(ethylene) distance of 2.020 Å. In contrast to the picture obtained for metallocene-based Ziegler−Natta catalysts,[33,34] there is no noticable agostic stabilization present in this transition state (propyl α-agostic Ni−H distance: 2.300

Å). After passing the transition state **TS[6a−10a]**, which lies 17.5 kcal/mol above **6a**, the complex decays into the thermodynamic insertion product **10a**.
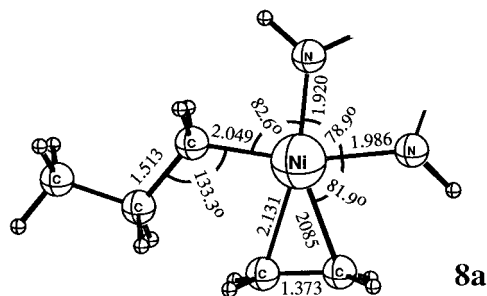

TS[6a-10a]

10a
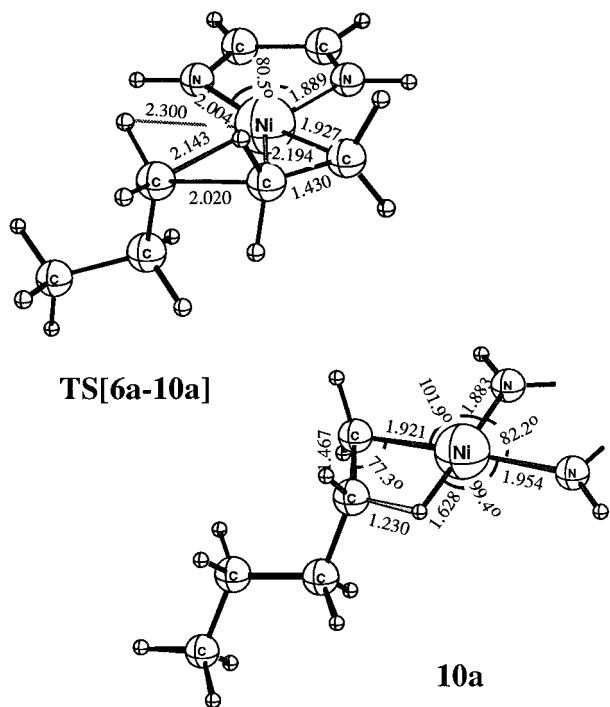
A second pathway proceeds entirely via C_s symmetric intermediates: shifting the ethylene moiety into the plane and displacing the β-agostic bond results in a square-planar intermediate **7a**, which has no agostic bonds and lies 6.5 kcal/mol above **6a**. The barrier for the reverse reaction **7a → 6a** in this case is very low (1.7 kcal/mol), so that the thermodynamic population of this isomer will be small. The transition state **TS[6a−7a]** associated with this process lies 8.2 kcal/mol above **6a**. The ethylene moiety can now rotate into the molecular plane to form **8a**, which lies 5.2 kcal/mol above **7a** due to incresed steric repulsion. As in the previous step, the transition state **TS[7a−8a]** has an almost identical energy with **8a** (barrier for the reverse reaction: 1.0 kcal/mol), so that analogously to **7a**, **8a** will be populated only sparsely. The actual insertion process occurs now via shrinkage of the C(propyl)$_\alpha$−C(ethylene) bond, leading to a transition state **TS[8a−9]** which lies 5.1 kcal/mol above **8a** and 16.8 kcal/mol above **6a**. The comparable total energies of **TS[6a−10a]** and **TS[8a−9]** suggest that in the insertion transition state, rotation of the propyl chain about the emerging propyl−olefin bond has a very low barrier. This picture is also supported by the fact that the C$_\beta$−C$_\gamma$ bond distance in **TS[8a−9]** (2.021 Å) is almost identical to the one found for **TS[6a−10a]** (2.020 Å). Also, the agostic bond strengths are equally negligible (propyl α-agostic Ni−H distances are 2.253 Å for **TS[8a−9]** and 2.300 Å for **TS[6a−10a]**). **TS[8a−9]** relaxes into a kinetic insertion product **9**, which exhibits strong η^2-γ-agostic bonding analogously to **4a**. The thermodynamic β-agostic product **10a** is reached via a transition state **TS[9−10a]**, which is analogous to **TS[4a−5a]** and lies only 2.7 kcal/mol above **9**.
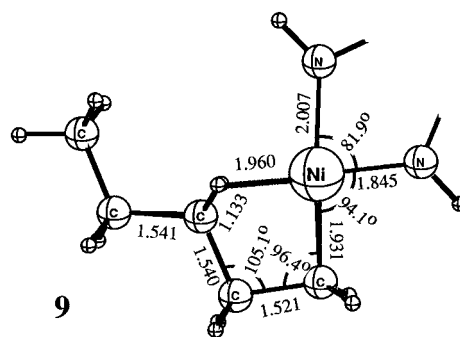
We conclude that the insertion process is exothermic by 6.7 kcal/mol relative to the π-complex **6a**, which is less than the 11.6 kcal/mol found for chain initialization. The difference of
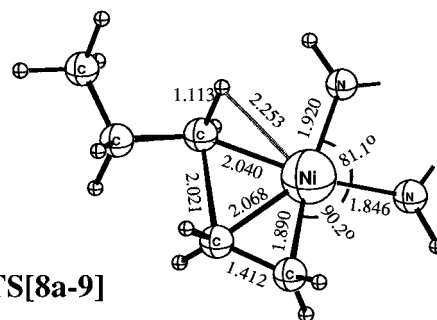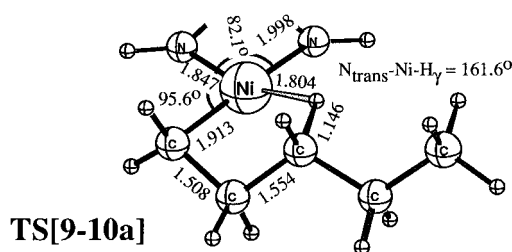
(33) Margl, P.; Lohrenz, J. C. W.; Ziegler, T.; Blöchl, P. E. *J. Am. Chem. Soc.* **1996**, *118*, 4434.

(34) Lohrenz, J. C. W.; Woo, T. K.; Ziegler, T. *J. Am. Chem. Soc.* **1995**, *117*, 12793.

7a

8a

9

TS[8a-9]

N_{trans}-Ni-H$_\gamma$ = 161.6°

TS[9-10a]

4.9 kcal/mol serves as an estimate of the bond strength of the residual β-agostic bond in **6a**. Since the bonding situations around the metal in **5a** and **10a** are extremely similar, we can verify the total reaction energy **5a** + C_2H_4 → **10a** of −26.1 kcal/mol by comparing it to estimates of the reaction energy based on standard tabulated values for the bond strengths.[35] The result (ADF, −26.1; tabulated experimental data, ca. −20 ± 4

(35) March, J. *Advanced Organic Chemistry. Reactions, Mechanisms, and Structure*; 4th ed.; John Wiley & Sons: New York, 1992.

kcal/mol) shows that our values for reaction energies are slightly overestimated. Taking into account the negligible populations of species **7a** and **8a** (due to the diminutive barrier for the reactions **7a** → **6a** and **8a** → **7a**) we reason that the effective barrier for insertion through the indirect channel must be very close to the energy difference between **TS[8a−9]** and **6a**, which puts it at ≈17 kcal/mol. Since the barrier for direct insertion is very similar (17.5 kcal/mol), we give a final, effective barrier for chain propagation of 17 kcal/mol. For comparison, the insertion of C_2H_4 into the Pd−ethyl bond of $H_2PCHCHCPH_2$-$Pd^{II}C_2H_5^+$ was calculated to proceed via a single-step mechanism, with a barrier of 15.5 kcal/mol.[24]

We also investigated the total energy of a number of other isomers close to the minimum energy pathway. If the initial attack of ethylene on **5a** occurs from the opposite face of the square-planar complex (i.e. *syn* relative to the terminal methyl group of the propyl chain), a trigonal bipyramidal complex **6b** is formed, which is analogous to **6a** except for increased steric repulsion between the olefin and the propyl chain ($E(\mathbf{6a})$ − $E(\mathbf{6b}) = -0.5$ kcal/mol). Conformers **7b** and **8b** are similar to **7a** and **8a** except for a 180° rotation of the propyl chain around the Ni−C_α bond, whereas in **10b**, the conformation of the C_γ−C_δ bond is gauche-staggered instead of anti-staggered as in **10a**. The total energies of isomers **6b**, **7b**, **8b**, and **10b** are given in Figure 3. Their minimum character was not confirmed in terms of the eigenvalues of the Hessian.

c. Chain Isomerization. Since the polymer produced by such catalysts as the one under investigation here can be highly branched,[1,2] with methyl branches predominating, we investigated the mechanism which allows chain isomerization. For isomerization to occur, a β-hydrogen has to be abstracted from the growing chain to form an olefin hydride complex. In such a complex, rotation of the chain about the Ni−olefin bond is supposed to be facile enough to allow reattachment of the hydride to the former α-carbon atom of the chain.

Starting from the β-agostic propyl complex **5a**, we model the isomerization process by a linear transit calculation, where we choose the torsion angle C_α−X−Ni−N (X denotes the C_α−C_β bond center) as a reaction coordinate. Our calculations showed that there is no stable minimum for a hydride−olefin complex, so that migration must proceed according to a concerted pathway, where dilation of the β-agostic bond and rotation of the olefin happen simultaneously. (Geometry optimization starting from a tentative olefin hydride complex inevitably leads to the β-agostic alkyl. A linear transit calculation with the alkyl-hydride distance as reaction coordinate shows monotonous increase of the energy as the C−H bond is stretched.) This is in agreement with previous calculations on a Pd(II) system, which showed that for $PH_2CHCHCPH_2Pd^{II}Et^+$, there is no stable minimum for an olefin hydride.[24] By linear transit and subsequent transition state optimization, we arrive at transition state **TS[5a−5b]** (Figure 4), which lies 12.8 kcal/mol above **5a**. In **TS[5a−5b]**, the β-agostic hydrogen is completely dissociated from the β-carbon atom (C_β−H distance = 2.246 Å), forming an olefin−hydrido framework with olefin and hydride each occupying one of the square-planar positions. The olefin is oriented approximately perpendicular to the molecular plane with C_α−C_β−Ni−H_β = 58.2°, with the internal carbon atom closer to the hydride than the terminal carbon atom. Further rotation directly yields the isomerization product **5b**, which has a β-agostic isopropyl chain and is 1.8 kcal/mol lower in energy than **5a**. This energetic stabilization of the isomerization product is important, since it would give rise to a completely branched polymer in the limit of thermodynamic control.
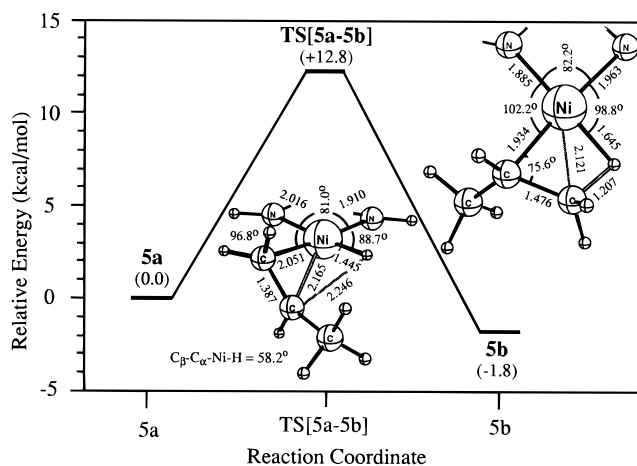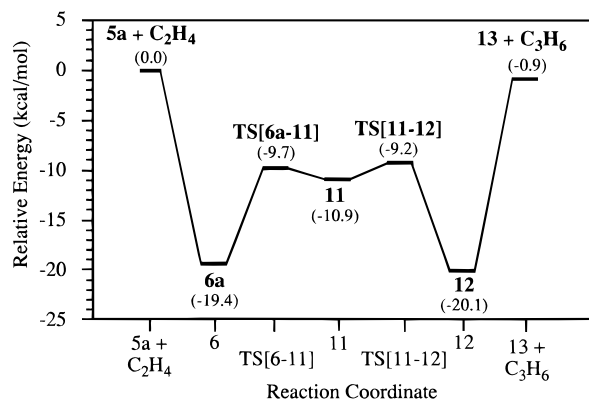

Figure 4. Energy profile for the chain-isomerization process. Conventions as in Figure 2.

d. Chain Termination. Long polymer chains can only be produced if the activation energy for chain termination is much larger than the activation energy for chain propagation. We therefore investigated the mechanism of chain termination, using a propyl group as a model for the growing chain. Starting from **6a**, we dilated the β-agostic C−H bond, arriving at **TS[6a−11]** (9.7 kcal/mol above **6a**). **TS[6a−11]** constitutes a transition

11

TS[6a-11]   **TS[11-12]**
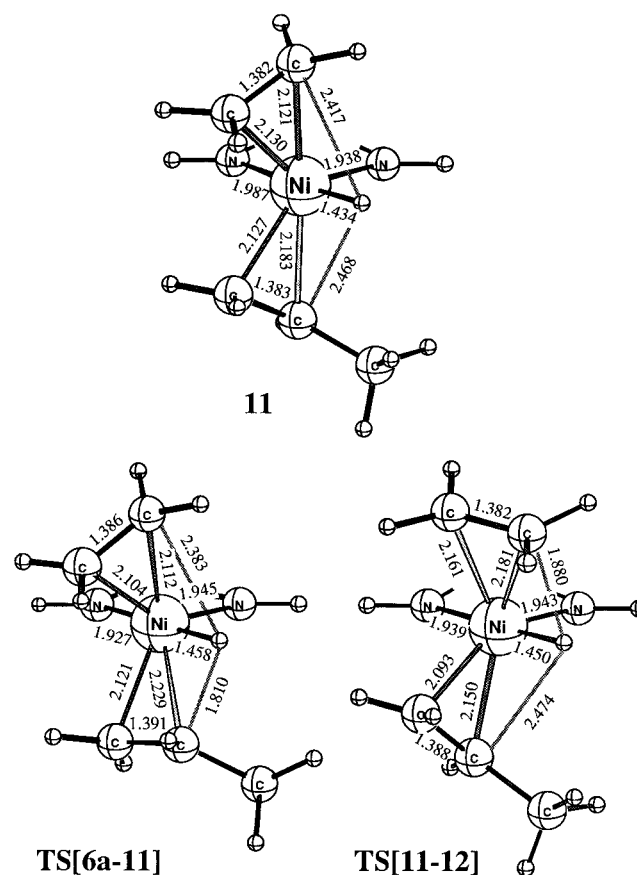
state with respect to hydride abstraction in the presence of a coordinated ethylene. Since the potential surface for this species is too flat to be tractable by a transition state search based on the Hessian, a fine-grid linear transit search was used to locate it. Only one degree of freedom was constrained during the linear transit calculation, therefore it is reasonably sure that **TS-[6a−11]** constitutes a true transition state. (The maximum component of the Cartesian gradient was 0.0006 au.) Further

Figure 5. Energy profile for the chain-termination process. Conventions as in Figure 2.

dilation of the C—H distance yields a stable hydride **11**, whose minimum character was confirmed by a frequency calculation which yielded no imaginary frequencies. This is in contrast to the finding that dilation of the β-agostic bond in **5a**, which has no additional ethylene in its coordination sphere, yields no stable hydride. However, the potential well for **11** is shallow (activation barrier for **11 → 6a**: 1.2 kcal/mol, Figure 5). Going further along the reaction coordinate yields a second transition state **TS[11−12]** (1.7 kcal/mol above **11**), which is analogous to **TS[6a−11]**. The chain termination product **12** lies 0.7 kcal/mol below **6a**. Reinsertion of the propene fragment of **12** into the Ni—ethyl bond would give rise to an ethyl branch in the growing chain. The vinyl-terminated chain can be expelled in a first-order reaction at an energetic cost of 19.2 kcal/mol to form the β-agostic ethyl complex **13**, which can add another ethylene to restart chain propagation. Note that the experimental entropy for C_2H_4 ejection is approximately 30 eu,[36] which corresponds to $\Delta G(\mathbf{12} \rightarrow \mathbf{13} + C_3H_6, 300K) = \Delta H + T\Delta S \approx 10$ kcal/mol. Therefore, dissociative chain displacement should be approximately as fast as chain termination in this system. Alternatively, the chain can be substituted by an incoming monomer by associative displacement, which has been shown experimentally to be an extremely fast process for open systems such as ours (footnote 12 in ref 2).

From the termination pathway as obtained above, it is possible to construct a three-step isomerization path whereby as a first step, the chain is terminated as described above (**7a → 12**). In the next step the chain rotates by 180°, followed by another termination process that reattaches the β-hydrogen to the previously terminated chain and completes the isomerization. Since rotation barriers for coordinated olefins are generally of the order of ≈5 kcal/mol for the present Ni system (**[TS7a−8a]**, **[TS2a−3a]**), the rate-determining process for this isomerization would be the termination steps involved. Based on the competitive speed of substitution reactions, however, we think it unlikely that the coordination lifetime of the terminated chain is long enough to allow for isomerization and a second termination to occur, although the possibility cannot be ruled out at this point. As a variation of this mechanism, one might consider not to complete the first termination but only to proceed to intermediate **11** and subsequently rotating the chain by 180°, while the hydrogen still occupies the hydride position. However, no transition state could be found for such a rearrangement since even a slight rotation of the terminated chain resulted in attachment of the hydride to the monomer and thus in chain termination. In the following section we will in detail discuss the relationship between theoretical and experimental results.

(36) Rix, F. C.; Brookhart, M.; White, P. S. *J. Am. Chem. Soc.* **1996**, *118*, 4746.
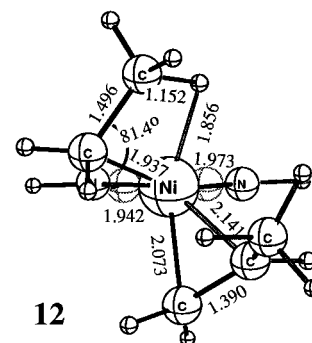
12
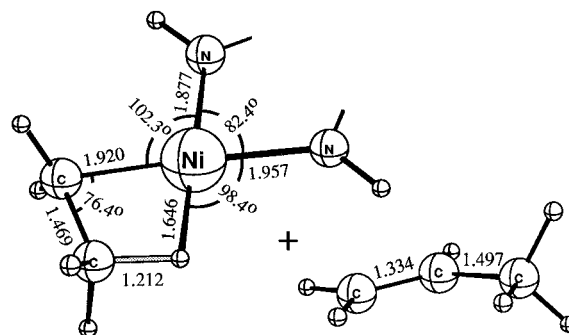
13 + C_3H_6

e. Comparison of Theoretical and Experimental Results. In previous studies, Brookhart and co-workers have shown that a Ni(II) center coordinated to an auxiliary ligand of the type Ar—N=C(R)—C(R)=N—Ar can efficiently catalyze the formation of high molecular weight polymers.[1,2] However, quantitative kinetic information is only available for the analogous Pd(II) model system.[2] We will in the following show how our results explain or conform with experimental data: *Experiment concluded that an alkyl—olefin complex is the catalyst resting state for both Pd(II) and Ni(II) centers.* This is confirmed by our calculations, which definitely show the π-complex **6a** to be the catalyst resting state since it is the most stable species on the potential surface (Figure 3). *For Pd(II) systems, experiment found an apparent activation free energy for the chain initialization of $\Delta G^{\ddagger} \approx 17$ kcal/mol.*[2] In good agreement with this experimental value, a diphosphine-coordinated Pd^{II}Et-(ethylene)$^+$ complex was previously shown by nonlocal DFT calculations to have a barrier of 15.5 kcal/mol for insertion of the olefin into the Pd(II)—ethyl bond.[24] Since there is no agostic bonding between ethyl and metal in the Pd(II) system, a Pd(II)—ethyl system behaves analogously to a Pd(II)—methyl system during olefin insertion. We find in this work an activation energy of 11.1 kcal/mol for the chain-initialization step in a Ni(II) system. The difference between the experimental value and the DFT result for Pd(II) on the one hand and the DFT result for Ni(II) on the other can be explained by the stronger π-bonding of ethylene to a Pd(II) center as compared to a Ni(II) center. *Experiment determined a barrier for chain propagation of ≈17−18 kcal/mol for Pd(II) systems.*[2] Chain propagation for our Ni(II) model has barriers of 17.5 and 16.8 kcal/mol, respectively, which are higher than the barrier for chain initialization. In contrast to this finding, experimental data gathered from the Pd(II) complex suggest that both chain initialization and propagation have about the same barriers. In our calculation, the increased barrier of propagation as compared to initialization is due to the strong β-agostic bonding in species **6a**, which gives additional stabilization to the educt state and therefore creates a higher barrier. Data from a previous DFT calculation show that for a Pd(II) system, no agostic bonding

exists in the educt state (see above). This nicely explains that the experimentally measured propagation barrier for a Pd(II) system is approximately identical to the initialization barrier, since both initialization and propagation educt states have no agostic bonds. *Since this is not the case for the Ni(II) system, the propagation barrier is significantly higher than the initialization barrier.*

Experimental molecular weights suggest that the barrier for chain termination in Ni(II) catalyst systems of this type with sterically demanding ligands is roughly 5 kcal/mol higher than that for chain propagation, which, added to our DFT propagation barrier, would put it at about 22 kcal/mol. The chain length of the polymer was observed to be dependent on the steric bulkiness of the Ar groups. A larger bulk corresponded to increased molecular weight.[2] Our barriers for chain termination ($\Delta H^{\ddagger} = 9.7$ kcal/mol) and subsequent ejection of the terminated chain ($\Delta G \approx 10$ kcal/mol) are in fact lower than the barrier for chain propagation. This means that a catalyst of the type investigated here, without additional steric bulk, would at best yield short oligomers. This agrees with the experimental fact that the sterically small (phenanthroline)Pd^{II}(Et)(C$_2$H$_4$)$^+$BAr$_4^-$ only dimerizes ethylene.[37] Since our transition states for chain termination are highly demanding with regard to space above and below the plane, steric bulk probably makes these transition state very unfavorable, thus giving rise to high molecular weight polymers due to suppressed chain termination. *For Ni(II) as well as Pd(II) systems, branching of the polymer can be regulated by changing the steric bulk of the auxiliary ligand. A bulkier auxiliary ligand corresponds to a more branched polymer.*[2] From the viewpoint of our calculations, two arguments serve to explain this: firstly, attack of C$_2$H$_4$ will be screened by the bulky ligand, thus effectively increasing the population of the isomerization precursor **5a** relative to the insertion precursor **6a**. Secondly, the energy difference between **5a** and **6a** will be reduced since **6a** will be energetically more unfavorable due to its large space demand, which again increases the population of **5a** relative to **6a**. *In experiments, a reduction of ethylene pressure increased the degree of branching in the chain.*[2] This is readily explained by the fact that increasing ethylene partial pressure reduces the population of **5a**, since more of the π-complex **6a** is formed. The experimentally observed branching frequency was approximately 1−100 branches per 1000 carbon atoms. This would suggest an isomerization barrier higher than the propagation barrier by 1−4 kcal/mol, which would put it at 18−21 kcal/mol. Our barrier for isomerization is 12.8 kcal/mol, which is in fact lower than the barrier for insertion. However, under experimental conditions, formation of **6a** serves as a sink which depletes population of

5a, thus effectively increasing the barrier for isomerization. A quantitative estimate of the apparent barrier from the viewpoint of our calculations is not straightforward and will not be attempted here, since it depends on a number of experimental factors which are not considered in our calculations.

Our results show that a very essential part of the catalyst's activity is indeed due to the careful choice of the auxiliary ligand, so that a detailed comparison can only be possible if this is included into the computational model. Calculations which taken into account the steric bulk of the auxiliary ligand are in progress at our laboratory.

4. Conclusion

We have studied the polymerization of ethylene with a Ni(II) catalytic center coordinated to diimide (HN═CH−CH═NH). We have investigated chain initialization and chain propagation as well as chain isomerization and chain termination. (i) Chain initialization proceeds in a stepwise fashion, with an overall activation barrier of 11.1 kcal/mol. (ii) Chain propagation can proceed via two different pathways, which have similar activation energies (16.8 and 17.5 kcal/mol, respectively). None of the insertion transition states shows agostic stabilization. (iii) The activation energy for chain isomerization is 12.8 kcal/mol, which proceeds via a concerted mechanism, rotating the chain and simultaneously abstracting the β-agostic hydrogen. Unlike suggested in the literature, no stable hydride is formed during chain isomerization. (iv) chain termination occurs in an associative fashion via a stable hydride intermediate, which is formed with a barrier of 9.7 kcal/mol and decays into the termination product with a small activation energy of 1.7 kcal/mol. (v) Production of experimentally observed high molecular weight polymers can only be explained by suppression of the chain termination transition state due to sterically demanding substituents on the diimine ligand, which was also postulated in the experimental literature.

Supporting Information Available: Cartesian coordinates of all species mentioned in the text (17 pages). See any current masthead page for ordering and Internet access instructions.

(37) Schmidt, G. F.; Brookhart, M. *J. Am. Chem. Soc.* **1985**, *107*, 1443.

JA962860E